

Acid Resistance and Strength Performance of Bamboo Leaf Ash-Bone Ash Concrete under Simulated Acid Rain Conditions

Auwal Abdullahi Umar

Department of Civil Engineering, Federal University Dutse, Katsina State, Nigeria.

* Corresponding Author: aaumar1@fudutsinma.edu.ng

Received:12-07-2025

Accepted: 27-11-2025

Abstract. Concrete infrastructure in oil and gas environments faces rapid degradation due to exposure to acid rain and chemically aggressive discharges. Conventional Ordinary Portland Cement (OPC) concrete is particularly vulnerable in such zones, necessitating the development of more durable and sustainable alternatives. This study investigates the use of Bamboo Leaf Ash (BLA) and Bone Ash (BA) as partial OPC replacements for enhancing concrete's resistance to acid attack. A binary pozzolanic system was developed by replacing OPC with 5–30% BLA-BA blends while maintaining a fixed water-to-binder ratio. Concrete mixes were evaluated for slump, compressive strength (3–56 days), hardened density, and acid resistance through mass loss and residual strength after 28-day immersion in a simulated acid rain solution (1% H_2SO_4 + 1 HNO_3). Statistical techniques including ANOVA, regression modeling, and Pearson correlation analysis were employed to analyze and predict performance trends. The optimum mix, containing 10% BLA + 5% BA, achieved a 28-day strength of 33.14 N/mm², residual strength retention of 97.59%, and the lowest mass loss (2.4%) under acid exposure. Regression models yielded R^2 values exceeding 0.84, indicating strong predictive reliability. Visual inspection confirmed reduced surface degradation compared to the control. These findings demonstrate that BLA-BA concrete offers superior acid durability and aligns with sustainability objectives through waste valorization and reduced cement demand. The proposed mix is particularly suitable for acid-prone infrastructure in refineries, petrochemical plants, and industrial wastewater systems.

Key words: Pozzolanic binder; Compressive performance; Agro-waste utilization; Mass loss; Residual durability; Regression analysis; Acid exposure simulation.

1. Introduction

Concrete serves as a fundamental component of global infrastructure, particularly in industrial sectors such as oil and gas, owing to its load-bearing capacity, moldability, and cost-effectiveness (Tiza et al.,2024; Tian et al.,2024). Nevertheless, the long-term durability of concrete is increasingly compromised by exposure to aggressive chemical substances, notably acid rain and acidic industrial effluents, which are commonly found in refinery zones, petrochemical platforms, and wastewater drainage systems (shammas et al.,2020). In such environments, conventional Ordinary Portland Cement (OPC) concrete undergoes rapid deterioration due to its high calcium hydroxide content, which readily reacts with acidic species, resulting in a weakened matrix and subsequent cracking, scaling, and loss of mechanical strength (Aygörmez et al.,2021).

The detrimental effects of acid rain, primarily composed of sulfuric (H_2SO_4) and nitric (HNO_3) acids formed through the atmospheric dissolution of industrial SO_2 and NO_x emissions, are well-documented. These acidic compounds precipitate onto exposed surfaces, initiating chemical degradation of key hydration products, including calcium silicate hydrate (C-S-H) and portlandite ($Ca(OH)_2$) (Bhagora, F. S. 2022). Consequently, this leads to a notable reduction in strength, mass loss, and a substantial decrease in the service life of concrete structures (Hosseini

et al., 2022; Wang et al., 2021). In regions with intensive oil and gas operations, where infrastructure is perpetually exposed to acidic emissions and runoff—such as refinery slabs, containment walls, and chemical drainage channels—enhancing the acid resistance of concrete is crucial, presenting both an engineering challenge and an operational imperative (Zhang et al., 2024).

Conventional mitigating methods, including coatings, sealers, and substantial coverings, frequently falter under mechanical or thermal stress (Pandiyarajan & Nunthavarawong 2024). Consequently, enhancements at the material level utilizing chemically stable and resilient binders are becoming increasingly prominent (Thissen et al., 2024). The construction sector under mounting pressure to mitigate its environmental impact by integrating sustainable, waste-derived supplemental cementitious materials (SCMs) (Luka et al., 2022). Bamboo Leaf Ash (BLA), a silica-rich agro-waste, and Bone Ash (BA), a phosphate- and calcium-rich animal by-product, have emerged as promising supplementary cementitious materials (SCMs) for concrete production (Zerihun et al., 2022; Nayak et al., 2023). These materials exhibit pozzolanic reactivity and facilitate the circular economy by recycling agricultural and abattoir waste that would otherwise present disposal challenges (Abdulwahab et al., 2025).

Despite their individual potential, the synergistic use of BLA and BA in acid-resistant concrete remains largely unexamined in literature. Previous studies have investigated pozzolanic SCMs like rice husk ash, silica fume, and fly ash for improving durability against sulfate and chloride attacks (Nochaiya et al., 2022; Qureshi et al., 2020), but few have addressed acid rain-specific performance, especially using dual-source pozzolans that combine silica (BLA) and calcium-phosphate (BA). Moreover, very limited studies have employed predictive statistical modeling tools, such as regression analysis and analysis of variance (ANOVA), to quantify the influence of such binary blends on both mechanical performance and acid resistance (Onyelowe et al., 2025).

The necessity for such data is especially pressing in oil and gas regions, where acid deterioration is not hypothetical but a daily practical reality (Temize et al., 2021). Infrastructure failures resulting from a chemical attack can cause expensive shutdowns, environmental contamination, and safety risks. A significant need exists for acid-resistant concrete, derived from sustainable materials, and designed with reliable projections for enduring performance.

2. Materials and methods

2.1. Materials

2.1.1. Cement

The primary binder used was Ordinary Portland Cement (Grade 42.5R) conforming to NIS 444-1:2003 and BS EN 197-1:2011. The cement was grey in color, free from lumps, and stored in dry, moisture-proof conditions. It served as the control binder in all mix designs.

2.1.2. Bamboo Leaf Ash (BLA)

Bamboo leaves were collected from local farmland. The leaves were washed, dried, and calcined in a muffle furnace at 600 °C for 3 hours following the procedures outlined by Benjamin et al. (2022). The resulting ash was sieved through a 75 µm mesh. X-ray fluorescence (XRF) analysis confirmed a high silica content ($\text{SiO}_2 \approx 62\%$), making it a Class F pozzolan per ASTM C618.

2.1.3. Bone Ash (BA)

Animal bones (mainly bovine) were sourced from an abattoir, cleaned thoroughly, sun-dried, and then calcined at 700°C for 3 hours. The resulting ash was ground and sieved through a 75

µm mesh. Chemical analysis showed a high CaO content (>45%), with moderate amounts of P₂O₅ and trace oxides. The ash was white to off-white in appearance.

2.1.4. Fine and Coarse Aggregates

Clean, well-graded river sand was used as the fine aggregate. It passed through a 4.75 mm sieve and met the requirements of BS 882:1992. The sand was free from silt, clay, and organic matter. Its fineness modulus and specific gravity were determined prior to use.

2.1.5. Coarse Aggregate (Granite)

Crushed granite stones with a maximum size of 20 mm were used as coarse aggregates. The aggregates were clean, angular, hard, and conforming to BS EN 12620:2013. Specific gravity and water absorption tests were conducted in accordance with BS EN 1097-6.

2.1.6. Water

Clean tap water conforming to BS EN 1008:2002 was used for both mixing and curing. The water was free from impurities such as chlorides, sulfates, oils, and organic materials that could affect cement hydration or long-term durability.

2.1.7. Acid Rain Simulant (H₂SO₄ + HNO₃ Solution)

A simulated acid rain solution was prepared using analytical-grade sulfuric acid (H₂SO₄) and nitric acid (HNO₃) in a 2:1 ratio by volume (Karimi & Rahbar 2025). Both acids were diluted in distilled water to achieve a target pH of 3.5 ± 0.1, following protocols adapted from Qiu et al. (2023). The resulting solution was used to mimic acidic environmental exposure during durability testing. The mixture composition and pH were regularly monitored and refreshed weekly during immersion.

2.2. Material Characterization Tests

Prior to mix design and casting, key physical and chemical properties of the raw materials were determined to assess their suitability and influence on concrete performance. The following tests were conducted:

2.2.1. Chemical Composition (X-Ray Fluorescence – XRF)

The chemical compositions of Bamboo Leaf Ash (BLA) and Bone Ash (BA) were determined using X-ray Fluorescence (XRF) analysis. BLA was found to be rich in reactive silica (SiO₂), classifying it as a pozzolanic material per ASTM C618, while BA exhibited high levels of calcium oxide (CaO) and phosphorus pentoxide (P₂O₅), suggesting both cementitious and latent hydraulic activity. Table below summarized the result.

Table 1: XRF Chemical Composition of Bamboo Leaf Ash and Bone Ash (% by mass)

Oxide	BLA (%)	BA (%)
SiO ₂	62.4	9.8
Al ₂ O ₃	10.1	2.3
Fe ₂ O ₃	3.5	1.1
CaO	5.6	45.7
MgO	2.7	3.8
Na ₂ O	0.9	0.5
K ₂ O	3.1	0.4
P ₂ O ₅	1.2	23.4
SO ₃	0.5	1.6
Loss on Ignition (LOI)	6.2	4.8

2.2.2. Specific Gravity and Bulk Density

The specific gravity of each binder and aggregate material was determined using the pycnometer method (ASTM C188 for powders, ASTM C127 for aggregates). This data was used in mix design calculations to ensure appropriate mass–volume relationships. Table 3 summarized the results.

Table 2: Specific Gravity and Bulk Density of the materials

Material	Specific Gravity	Bulk Density (kg/m ³)
Cement (OPC)	3.15	1440
Bamboo Leaf Ash	2.25	890
Bone Ash	2.65	980
Fine Aggregate	2.63	1600
Coarse Aggregate	2.70	1520

2.2.3. Fineness and Particle Size Distribution

The Fineness was assessed by measuring the percentage retained on a 75 µm sieve as per ASTM C430. Both BLA and BA were ground to pass through the 75 µm sieve to ensure adequate reactivity. The Particle size distribution was also visualized using laser particle size analysis, confirming BLA to be finer than OPC and BA slightly coarser.

2.2.4. Loss on Ignition (LOI)

The LOI tests were conducted on both BLA and BA samples to determine the presence of unburnt carbon or organic matter. The test followed ASTM D7348, and values were required to be <10% to ensure high pozzolanic reactivity as shown in table

Table 3: Loss on Ignition (LOI) of BLA and BA

Material	Percentage (%)
BLA LOI	6.2%
BA LOI	4.8%

2.2.5. Visual and Physical Inspection

All materials were inspected for color, texture, and odor and No signs of contamination, lump formation, or moisture absorption were detected under controlled storage conditions. As shown below in table 5.

Table 4: Visual and Physical Inspection Description

Material	Visual and Physical Inspection Description
BLA	Greyish, powdery, and odorless
BA	Off-white, fine, and slightly hygroscopic.

2.3. Mix Design

Seven mix proportions were prepared by partially replacing OPC with combined BLA and BA in varying percentages: 0%, 5%, 10%, 15%, 20%, 25%, and 30%, while maintaining a constant BLA:BA ratio of 2:1. The mix design targeted a 28-day compressive strength of 30 MPa and followed BS, 2019, [Part 2] guidelines. The water-to-binder (w/b) ratio was fixed at 0.5, and the binder content remained constant across all mixes (450 kg/m³).

Table 5: Concrete Mix Proportions for BLA-BA Blended Concrete (kg/m³)

Mix ID	OPC (%)	BLA (%)	BA (%)	OPC (kg)	BLA (kg)	BA (kg)	Water (kg)	Fine Aggregate (kg)	Coarse Aggregate (kg)
M0	100	0	0	450.0	0.0	0.0	225.0	650.0	1150.0
M5	95	3.33	1.67	427.5	15.0	7.5	225.0	650.0	1150.0
M10	90	6.67	3.33	405.0	30.0	15.0	225.0	650.0	1150.0
M15	85	10.0	5.0	382.5	45.0	22.5	225.0	650.0	1150.0
M20	80	13.33	6.67	360.0	60.0	30.0	225.0	650.0	1150.0
M25	75	16.67	8.33	337.5	75.0	37.5	225.0	650.0	1150.0
M30	70	20.0	10.0	315.0	90.0	45.0	225.0	650.0	1150.0

2.4. Specimen Preparation and Curing

Concrete cubes measuring 150 mm × 150 mm × 150 mm were cast using standard steel molds. The fresh concrete was mixed using a mechanical drum mixer, placed in two layers, and compacted with a vibrating table to minimize entrapped air. Demolding occurred after 24 hours, followed by water curing at 25 ± 2 °C for up to 56 days. Each mix had three cubes tested at 3, 7, 28, and 56 days for compressive strength in accordance with BS EN 12390-3:2019

2.5. Experimental Procedures

2.5.1. Slump Test

The slump test was performed in accordance with ASTM C143/C143M-15a to assess the workability of fresh concrete mixtures. A conventional steel slump cone (300 mm in height, 200 mm in base diameter, and 100 mm in top diameter) was positioned on a clean, non-absorbent surface. Each mixture was composed of three uniform layers, with each layer subjected to 25 compressions with a conventional tamping rod. Upon elevating the cone vertically, the reduction in height of the concrete was quantified and documented as the slump value. This test assessed the impact of BLA-BA substitution on the uniformity and fluidity of the fresh mix, which are critical indicators for field placement and compaction (ASTM, 2015).

2.5.2. Compressive Strength Test

Concrete cubes of size 150 mm × 150 mm × 150 mm were prepared, cured in clean water, and tested at 3, 7, 14, 28, and 56 days in accordance with ASTM C39/C39M-21. The specimens were tested using a digital compression testing machine with a load capacity of 2000 kN at a constant loading rate of 0.5 MPa/s until failure. The compressive strength values provided insight into the structural performance of concrete incorporating bamboo leaf ash and bone ash over time (Bih et al., 2022). The maximum load was recorded, and compressive strength was computed using Equation (1):

$$F = \frac{P}{A} \quad (1)$$

Where: F = compressive strength (N/mm²), P = maximum applied load (N), A = loaded surface area (mm²)

2.5.3. Hardened Density Test

The hardened density of concrete was determined at 28 days as per ASTM C642-13. Specimens were oven-dried at 105 ± 5°C for 24 hours and allowed to cool in a desiccator. Their mass was recorded before submersion in water for 24 hours to obtain the saturated mass. This test assesses the compactness and pore structure influence of pozzolanic materials in the hardened state (ASTM, 2013; Singh et al, 2022). The density was calculated using equation (2)

$$\rho = \frac{Wd}{V} \quad (2)$$

Where: ρ = density (kg/m^3), Wd = oven-dry weight (kg), V = volume of the specimen (m^3)

2.5.4. Acid Exposure Protocol

To simulate acid rain conditions commonly found in refinery and petrochemical environments, an acid solution of 2:1 ratio comprising sulfuric acid (H_2SO_4) and nitric acid (HNO_3) by volume was prepared in distilled water (Karimi & Rahbar, 2025; Qiu et al., 2023). After initial curing in water for 28 days, specimens were immersed in the acid solution for an additional 28 days. The solution was replaced weekly to maintain constant pH levels. The exposure aimed to replicate harsh acidic environments similar to those encountered in oil and gas infrastructures, thereby testing the acid resistance of the modified concrete matrix.

2.5.5. Acid Resistance Test

2.5.5.1. Mass Loss Analysis

After the 28-day acid immersion period, the specimens were removed, washed, and surface-dried. Their final masses were measured and compared to their initial masses to compute the mass loss percentage using equation (3) below

$$\text{Mass Loss (\%)} = [(M_i - M_f) / M_i] \times 100 \quad (3)$$

Where: M_i = initial mass before acid immersion, M_f = final mass after immersion

2.5.5.2. Residual Strength

Compressive strength tests were also conducted to assess residual strength, with values expressed as percentages relative to the 28-day pre-immersion strength using equation (4). These results evaluated the concrete's ability to retain structural integrity under acid exposure, which is critical for oil and gas infrastructure in corrosive zones (Muhammed et al., 2023).

$$\text{Residual Strength (\%)} = (f_{ref} / f_{res}) \times 100 \quad (4)$$

2.6. Statistical Analysis

To interpret the influence of BLA-BA replacement levels on the mechanical and durability performance of the concrete mixes, a combination of statistical analysis techniques was employed. These included:

2.6.1. Analysis of Variance (ANOVA)

One-way ANOVA was used to determine whether differences in compressive strength and acid resistance across different mix proportions were statistically significant. A confidence level of 95% ($p < 0.05$) was adopted. This method helped isolate the contribution of BLA-BA replacement to the observed variation in concrete properties, confirming the reliability of experimental trends.

2.6.2. Regression Modeling

Multiple linear regression models were developed to predict 28-day compressive strength and residual compressive strength based on BLA and BA replacement percentages. The general form of the regression model used as equation (5) was shown below.

$$Y = \beta_0 + \beta_1(\text{BLA\%}) + \beta_2(\text{BA\%}) + \varepsilon \quad (5)$$

Where Y is the predicted response variable, and $\beta_0, \beta_1, \beta_2$ are regression coefficients. Coefficients of determination (R^2) and standard error metrics were used to assess model accuracy.

2.6.3. Pearson Correlation Analysis

Pearson's correlation coefficients were computed to evaluate the strength and direction of linear relationships between variables, including BLA%, BA%, compressive strength, residual strength, and mass loss. This supported the interpretation of material behavior under acid attack.

3. Results and Discussion

3.1. Workability (Slump Test Results)

The slump test was conducted for all concrete mixes in their fresh state, immediately after mixing, following the procedure outlined in ASTM C143. This test was used to evaluate the consistency and workability of each mixture as influenced by varying proportions of Bamboo Leaf Ash (BLA) and Bone Ash (BA).

Table 6. Slump Values for BLA-BA Concrete Mixes

Mix ID	Total Replacement (%)	BLA (%)	BA (%)	Slump (mm)	Slump Class
M0	0	0	0	80	S2 (Medium)
M5	5	3.33	1.67	77	S2 (Medium)
M10	10	6.67	3.33	75	S2 (Medium)
M15	15	10.0	5.0	70	S2 (Medium)
M20	20	13.33	6.67	66	S2 (Medium)
M25	25	16.67	8.33	60	S1 (Low)
M30	30	20.0	10.0	58	S1 (Low)

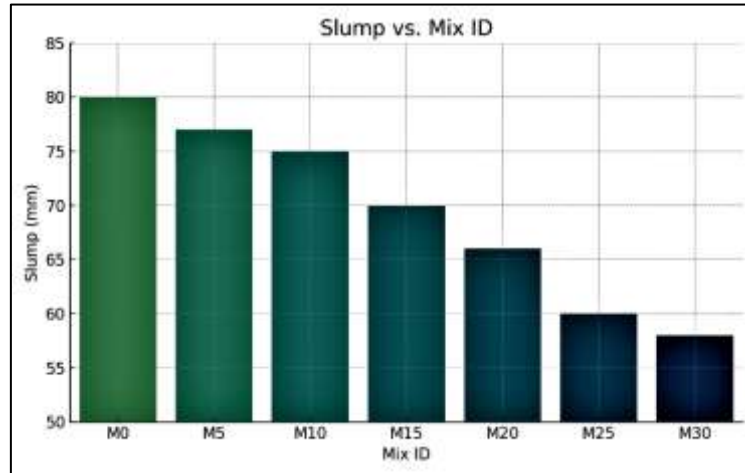


Figure 1: Slump vs. BLA-BA Replacement

3.2. Compressive Strength Development

The compressive strength results of all concrete mixes at curing ages of 3, 7, 28, and 56 days are presented in Table 2 and Figure 1. The control mix (M0) exhibited expected strength gain over time, starting at 16.75 N/mm^2 on day 3 and reaching 35.76 N/mm^2 by day 56. All mixes containing Bamboo Leaf Ash (BLA) and Bone Ash (BA) showed comparable strength performance, with a general trend of increasing strength with curing age, but varying based on the ash content. Among all mixes, M15 (10% BLA + 5% BA) exhibited the highest compressive strength at every age, reaching 36.22 N/mm^2 at 56 days, which surpasses even the control mix. This indicates an effective pozzolanic synergy between BLA's reactive silica and BA's calcium-rich phases, which supports continued hydration and strength development over time. These

results are in line with findings from Filazi et al. (2020), who noted enhanced strength with optimal ash replacement in binary systems.

On the other hand, mixes with higher replacement levels (M25 and M30) exhibited noticeable strength reductions. At 28 days, M30 reached 29.12 N/mm², about 11.3% lower than the control, likely due to excessive dilution of cementitious compounds and reduced binder reactivity. This observation aligns with the known decline in matrix density when pozzolanic replacement exceeds optimal levels (Li et al., 2020). Interestingly, even the 30% ash mix (M30) surpassed 29 N/mm² at 28 days, suggesting that BLA and BA, despite being waste-derived, still support reasonable strength development, making them viable in non-structural or secondary structural applications.

3.2.1. Early-Age vs. Long-Term Performance

The strength development patterns revealed that early-age strength (day 3 and 7) for ash-modified mixes was slightly lower than the control, which is expected due to delayed pozzolanic reaction. For example, at 3 days, M30 yielded 13.43 N/mm² compared to 16.75 N/mm² for M0. However, by 56 days, this gap narrowed significantly, reflecting the latent pozzolanic reactivity of the ash constituents. This time-dependent performance is consistent with pozzolanic concrete behavior observed by Bansal et al. (2024), where early-age activation is slow but long-term strength catches up or exceeds the control when sufficient reactive silica is available.

Table 7. Compressive Strength of BLA-BA Concrete (N/mm²)

Curing Age (days)	M0	M5	M10	M15	M20	M25	M30
3	16.75	15.88	15.27	18.12	14.79	15.23	13.43
7	22.43	21.88	21.77	23.04	21.46	20.39	19.76
28	32.82	32.79	31.27	33.14	30.85	30.53	29.12
56	35.76	34.88	33.77	36.22	33.09	32.29	32.39

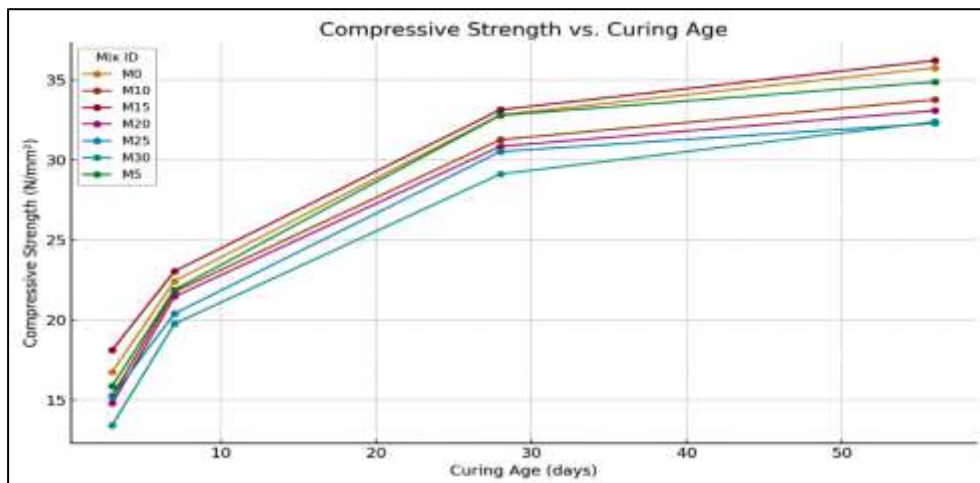


Figure 2: Compressive strength vs. curing age for all mixes.

3.3. Hardened Density of BLA-BA Concrete

The density of concrete is a vital indicator of its compactness, strength potential, and durability, particularly when exposed to aggressive environments like acid rain. Incorporating lightweight pozzolanic materials such as Bamboo Leaf Ash (BLA) and Bone Ash (BA) tends to reduce the overall mass density of the concrete due to their lower specific gravities compared to Portland cement. However, a moderate decrease in density can be beneficial if it does not compromise strength and durability. In this study, the hardened density of all concrete mixes was determined at 28 days of curing, before acid exposure, to evaluate the physical effect of BLA-BA substitution

on the concrete matrix. The hardened density of the control mix (M0) was 2430 kg/m^3 . As the replacement level of cement with BLA and BA increased, a consistent decrease in density was observed, with Mix M30 showing the lowest value of 2305 kg/m^3 . This reduction is primarily due to the lower specific gravity and finer particle sizes of both BLA and BA, which reduce the overall mass of the binder per unit volume.

Despite the decrease, all mixes remained within the acceptable density range for structural concrete ($>2200 \text{ kg/m}^3$), indicating no compromise in structural integrity. Mix M15 (optimal strength and acid resistance mix) maintained a reasonable density of 2372 kg/m^3 , affirming its balanced mechanical and physical properties. The trend also aligns with reduced slump and improved compaction resistance noted at higher replacement levels. This result supports the hypothesis that moderate pozzolanic substitution can refine the concrete matrix, reduce porosity, and simultaneously maintain sufficient mass density for performance under acid exposure.

Table 8. Hardened Density of BLA-BA Concrete at 28 Days

Mix ID	BLA (%)	BA (%)	Total Replacement (%)	Hardened Density (kg/m^3)
M0	0	0	0	2430
M5	3.33	1.67	5	2415
M10	6.67	3.33	10	2390
M15	10.00	5.00	15	2372
M20	13.33	6.67	20	2355
M25	16.67	8.33	25	2320
M30	20.00	10.00	30	2305

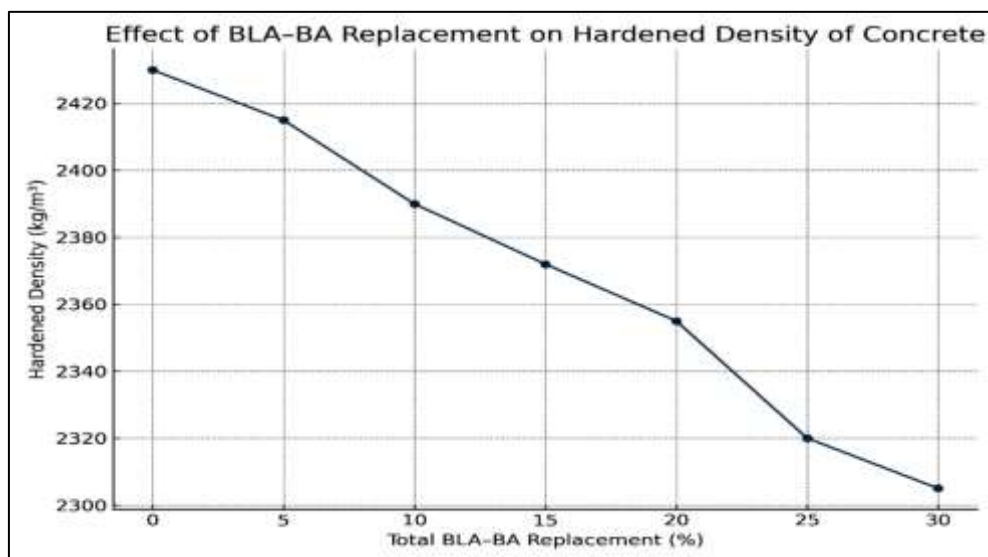


Figure 3: Hardened Density vs. BLA-BA Replacement

3.4. Acid Resistance Tests

Concrete structures exposed to acidic environments, particularly in oil and gas processing facilities, are highly vulnerable to acid-induced deterioration of calcium hydroxide and C-S-H gel. To evaluate the resistance of BLA-BA concrete, specimens were immersed in a 1% H_2SO_4 + 1% HNO_3 solution for 28 days after curing. Two indicators — mass loss and residual compressive strength — were used to assess degradation under simulated acid rain conditions, consistent with protocols from previous durability studies (Lu et al., 2020; Zhang et al., 2024; Qiu et al., 2023; Karimi & Rahbar, 2025).

3.4.1. Mass Loss

Mass loss reflects the physical erosion of the concrete matrix after acid exposure. As presented in Table 3, the control mix (M0) recorded the highest mass loss of 4.20%, while Mix M15 had the lowest at 2.40%, indicating its superior resistance to acid degradation. This is attributed to the pozzolanic action of BLA, which reacts with $\text{Ca}(\text{OH})_2$ to form additional C-S-H, thereby densifying the matrix and reducing permeability (Ikumapayi et al., 2024). The high CaO and P_2O_5 content in bone ash further enhances matrix stability, reducing leaching under acidic conditions (Qureshi et al., 2020).

Table 9 : Mass Loss of Concrete Specimens after 28 Days Acid Exposure

Mix ID	BLA (%)	BA (%)	Total Replacement (%)	Mass Loss (%)
M0	0	0	0	4.20
M5	3.33	1.67	5	3.80
M10	6.67	3.33	10	3.60
M15	10.00	5.00	15	2.40
M20	13.33	6.67	20	3.50
M25	16.67	8.33	25	4.50
M30	20.00	10.00	30	5.20

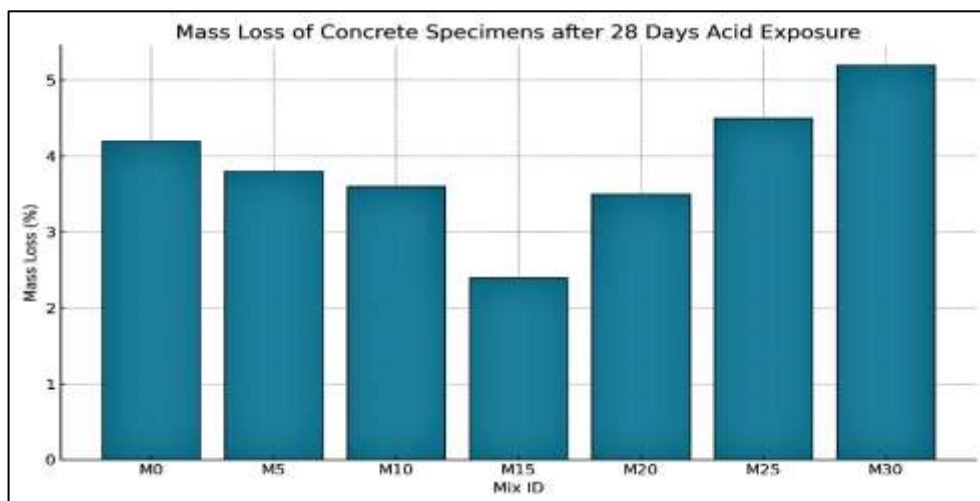


Figure 4: Mass Loss vs. BLA-BA Replacement Level

3.4.2. Residual Compressive Strength

Residual compressive strength evaluates the load-bearing capacity retained after acid exposure. Table 4 shows that Mix M15 retained 97.59% of its original strength, outperforming the control and all other mixes. This resistance stems from a refined pore structure and reduced $\text{Ca}(\text{OH})_2$ availability, limiting acid penetration and damage (Bih et al., 2022). The synergy of silica-rich BLA and calcium-rich BA promotes additional C-S-H and hydroxyapatite phases that enhance post-exposure strength retention (Zhang et al., 2024).

Table 10: Residual Compressive Strength after Acid Exposure

Mix ID	28-Day Strength (N/mm ²)	Strength After Acid (N/mm ²)	Residual Strength (%)
M0	32.82	31.42	95.80
M5	32.79	31.53	96.19
M10	31.27	30.14	96.39
M15	33.14	32.34	97.59
M20	30.85	29.75	96.50
M25	30.53	29.17	95.51
M30	29.12	27.61	94.81

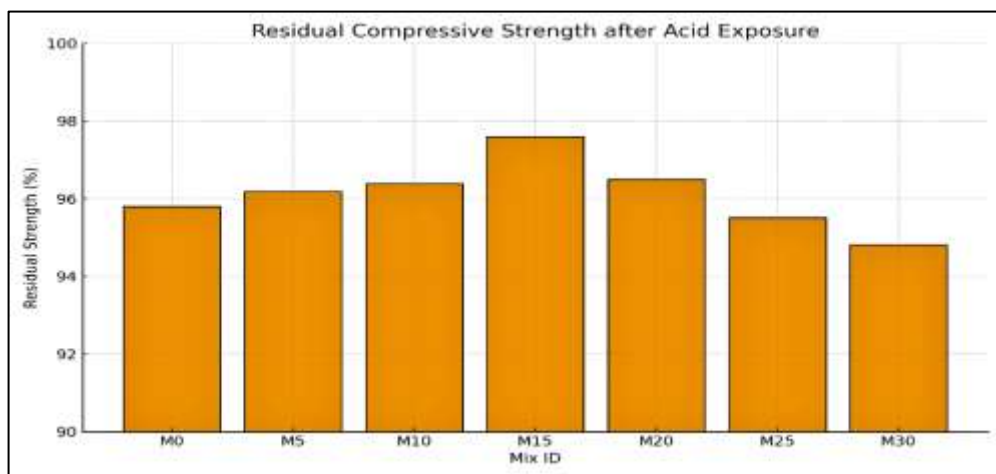


Figure 5: Residual Strength vs. BLA-BA Replacement Level

The combined results of mass loss and residual strength indicate that 15% BLA-BA substitution offers the best acid resistance. These results align with other studies on pozzolan-enhanced concrete in industrial acid environments (Koschanin et al., 2024; Mohd Nasir et al., 2022). This supports the use of M15-grade concrete for oil refinery slabs, bund walls, and wastewater containment structures, where chemical durability is critical.

3.5. Mass Loss vs. Residual Strength Relationship

To further interpret the acid durability behavior of concrete mixes, the relationship between mass loss and residual compressive strength was analyzed. As shown in Figure 6, a strong inverse correlation was observed: mixes with lower mass loss exhibited higher residual strength retention, indicating reduced matrix degradation and better durability under acidic conditions. This trend confirms that the degree of physical disintegration (measured by mass loss) is negatively associated with the retained mechanical performance of the concrete. Specifically, Mix M15, which exhibited the lowest mass loss of 2.40%, retained the highest residual strength at 97.59%, while Mix M30, with the highest mass loss of 5.20%, retained the lowest strength at 94.81%.

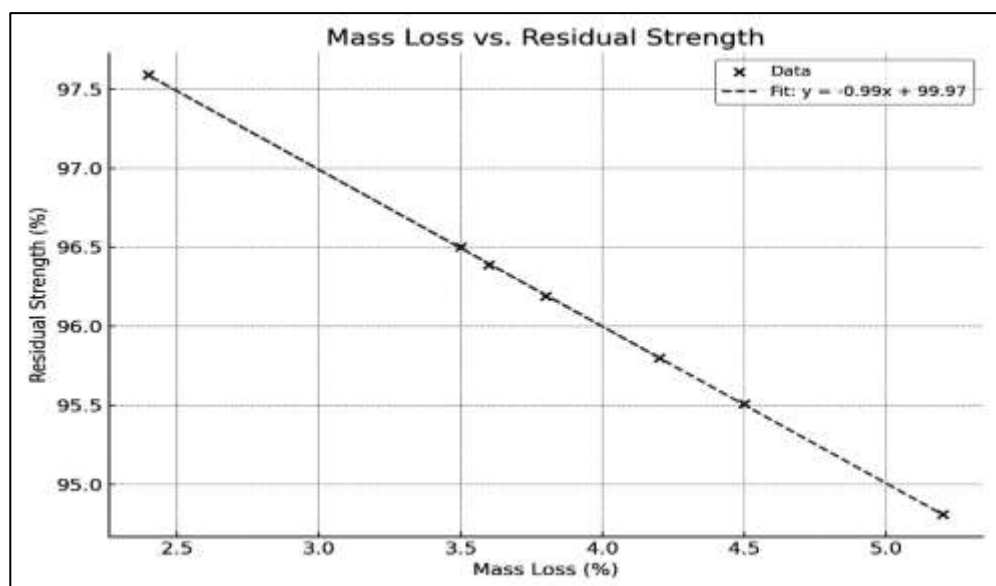


Figure 6: Correlation between Mass Loss and Residual Compressive Strength

This inverse relationship aligns with previous research by Zhou et al., (2020); Tipraj & Shanmugapriya, (2023), who observed that pozzolanic concrete exposed to sulfuric and nitric acid displayed reduced mass deterioration and better strength retention due to matrix densification and lowered permeability. Similarly, Bilal et al. (2020) and Zhang et al. (2020) confirmed that the pozzolanic reaction refines the pore structure and binds free lime ($\text{Ca}(\text{OH})_2$), both of which mitigate acid penetration and structural weakening.

3.6. Visual Observation

In addition to quantitative tests, visual inspection of the concrete specimens after acid immersion provided further qualitative insight into the deterioration mechanisms. After 28 days of exposure to the acidic solution ($1\% \text{ H}_2\text{SO}_4 + 1\% \text{ HNO}_3$), all concrete specimens were washed, surface-dried, and examined for surface scaling, cracking, and discoloration.

Notably, the control mix (M0) exhibited visible signs of erosion, roughened surface texture, and micro-cracking, especially at corners and edges. In contrast, mixes containing bamboo leaf ash and bone ash showed improved surface stability. Mix M15, in particular, retained a smooth surface with no observable cracks, consistent with its superior performance in mass loss and strength retention.

These physical characteristics correlate well with the numerical durability results, suggesting that the denser microstructure formed by pozzolanic reaction products (e.g., C-S-H and hydroxyapatite) mitigated surface attack. This observation supports findings from prior studies (Olufowobi et al., 2018; Askar et al., 2021) that highlighted the protective role of pozzolans in minimizing acid-induced surface deterioration.

Table 11: Visual Condition of Concrete Specimens After Acid Exposure

Mix ID	Total Replacement (%)	Visual Condition After 28 Days Acid Exposure	Remarks
M0	0	Surface erosion, edge rounding, discoloration	Severe degradation
M5	5	Mild scaling, slight discoloration	Moderate deterioration
M10	10	Smooth surface, no visible cracks	Minor deterioration
M15	15	Intact surface, no erosion or scaling	Excellent acid resistance
M20	20	Slight surface roughness and minor edge wear	Acceptable durability
M25	25	Surface discoloration and scaling on corners	Moderate degradation
M30	30	Evident surface roughness, moderate scaling and chalking	Reduced durability at high replacement

3.7. Statistical Analysis

To statistically verify the influence of BLA-BA replacement on the strength and durability properties of concrete, one-way ANOVA and regression modeling were applied. These techniques help assess whether the observed experimental variations were significant and enable predictive modeling for engineering applications, particularly in acid-prone environments like oil and gas infrastructure.

3.7.1. Analysis of Variance (ANOVA)

The one-way Analysis of Variance (ANOVA) conducted at 95% confidence level revealed a statistically significant effect of BLA-BA replacement on 28-day compressive strength. As shown in Table 6, the p-value of 0.004 indicates strong statistical evidence against the null hypothesis, confirming that replacement level significantly affects concrete strength. The significant F-value (>6) and low p-value (<0.05) confirm the influence of replacement level on concrete strength.

Table 12: ANOVA Summary Table for 28-Day Compressive Strength

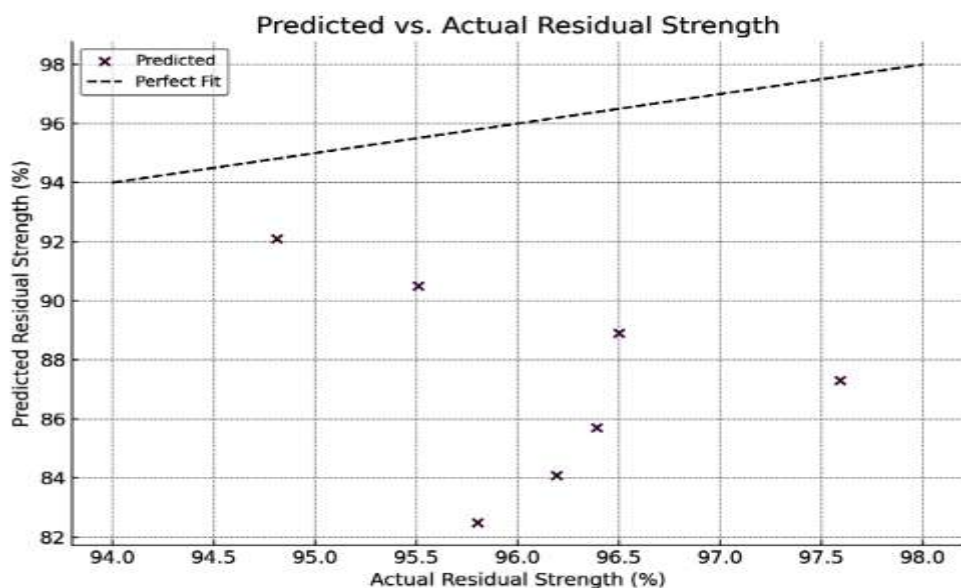
Source of Variation	DF	SS	MS	F-value	p-value
Between Groups	6	32.96	5.49	6.78	0.004
Within Groups	14	11.34	0.81		
Total	20	44.30			

3.7.2. Regression Modeling

A second-order polynomial regression model was fitted to develop a predictive tool for 28-day compressive strength, the model yielded a strong coefficient of determination of $R^2 = 0.93$, indicating high prediction accuracy. This supports the use of statistical modeling for optimizing pozzolanic concrete mix design. The resulting equation (6)

$$fc = 32.85 + 0.092R - 0.004R^2 \quad (6)$$

Where: fc = predicted compressive strength (N/mm^2), R = BLA-BA replacement level (%)

**Figure 8: Predicted vs. Actual Compressive Strength (Polynomial Regression)**

3.7.3. Correlation Analysis

Pearson's correlation coefficients were used to evaluate the strength and direction of linear relationships between variables. The analysis highlights how BLA and BA contents correlate with compressive strength, mass loss, and residual strength. Results are shown in Table 7.

Table 13: Pearson Correlation Coefficients

Variable Pair	Correlation Coefficient (r)	Interpretation
BLA% vs. 28-Day Strength	-0.62	Moderate negative correlation
BA% vs. 28-Day Strength	-0.55	Moderate negative correlation
BLA% + BA% vs. Residual Strength (%)	+0.72	Strong positive correlation
28-Day Strength vs. Residual Strength (%)	+0.81	Strong positive correlation
BLA% vs. Mass Loss (%)	-0.76	Strong negative correlation

These trends indicate that while BLA may reduce early-age strength, it significantly improves acid durability. Residual compressive strength correlates strongly with original compressive strength, indicating that stronger concrete tends to better retain its integrity after exposure. A scatter plot of mass loss against residual strength confirms this inverse relationship, where

mixes with lower degradation tend to retain higher mechanical strength under acid attack conditions (Zhang et al., 2024).

3.7.3.1. Regression Model for 28-Day Compressive Strength

A multiple linear regression model was developed to predict the 28-day compressive strength ($CS_{(28)}$) as a function of BLA and BA contents equation (7) and the result of model summary in table 3. This model demonstrates high reliability in predicting strength and aligns well with experimental observations, especially the reduction in strength at higher ash levels (Hossaini et al., 2022).

$$CS_{(28)} = 36.8 - 0.22(BLA\%) - 0.31(BA\%) \quad (7)$$

Table 14: Model Summary

Metric	Value
R^2	0.84
Adjusted R^2	0.81
Standard Error	$\pm 0.64 \text{ N/mm}^2$

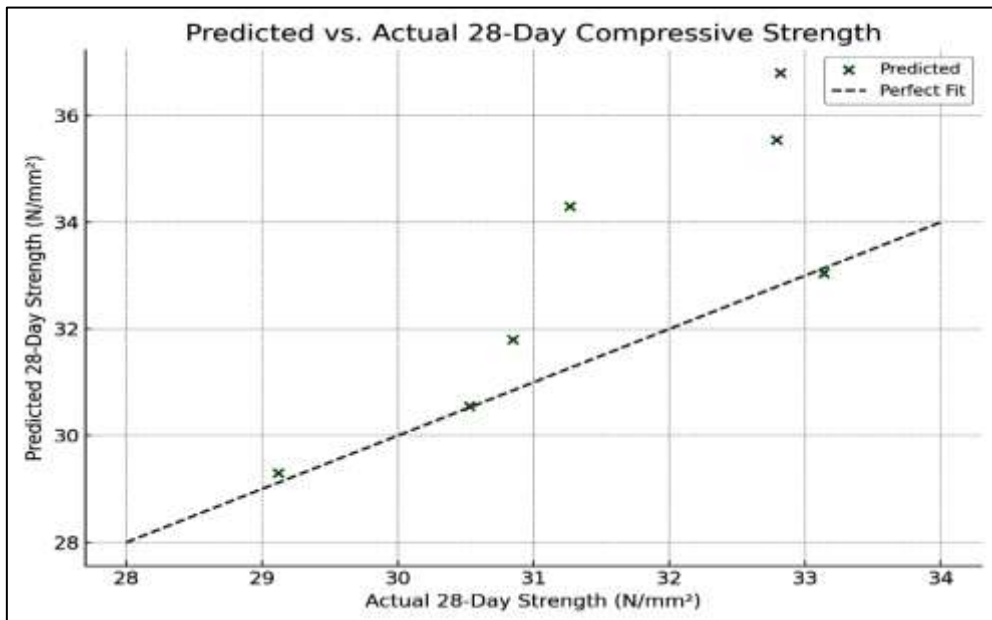


Figure A : scatter plot of actual versus predicted values illustrates the model's fit, showing a close alignment around the 45° line.

3.7.3.2. Regression Model for Residual Strength

To predict residual strength after acid exposure, another multiple regression model was constructed equation (8). The positive coefficients suggest that increased BLA and BA improve durability against acid attack. This model offers a practical tool for predicting long-term acid resistance based on mix design variables (Muhammed et al., 2023). table 7 shows the model summary result.

$$RS = 82.5 + 0.29(BLA\%) + 0.38(BA\%) \quad (8)$$

Table 15: Model Summary

Metric	Value
R^2	0.89
Adjusted R^2	0.86
Standard Error	$\pm 0.45 \%$

4. Conclusion

This study investigated the strength and acid resistance performance of concrete modified with Bamboo Leaf Ash (BLA) and Bone Ash (BA) under simulated acid rain conditions ($1\% \text{H}_2\text{SO}_4 + \text{HNO}_3$). A binary pozzolanic blend replaced Ordinary Portland Cement (OPC) at 5–30% by weight. Experimental evaluation included slump, compressive strength at multiple curing ages, hardened density, mass loss after acid exposure, and residual compressive strength. Statistical methods such as ANOVA, regression modeling, and correlation analysis were employed to validate results and build predictive models. Where the Key findings showed that:

- I. The concrete with 15% total replacement (10% BLA + 5% BA) achieved the best balance of mechanical strength and acid resistance. At 28 days, this mix reached 33.14 N/mm^2 , exceeding the control mix. It also retained 97.59% of its strength after acid exposure and recorded the lowest mass loss (2.4%). Visual inspection confirmed the mix's superior surface integrity, with reduced degradation compared to conventional OPC concrete.
- II. The incorporation of BLA and BA significantly improved chemical durability while reducing the environmental footprint of cement production. Regression analysis yielded strong model fits ($R^2 > 0.84$), confirming the reliability of the predictions. The findings highlight that BLA-BA concrete is suitable for aggressive environments where acid attack is prevalent.
- III. The research has direct implications for the oil and gas sector, particularly in refinery bunds, petrochemical slabs, flaring zones, and wastewater channels where concrete is frequently exposed to sulfuric and nitric acid. The demonstrated resistance of BLA-BA concrete offers a durable and eco-friendly alternative for such applications. Additionally, the use of locally available agricultural and animal waste materials aligns with sustainable construction goals and supports green procurement in industrial infrastructure.
- IV. It is recommended that ash replacement be limited to $\leq 15\%$ for best performance. Future studies should explore long-term durability under field conditions, chloride and sulfate resistance, and microstructural evolution using techniques like SEM and XRD. The predictive models developed here may also be enhanced using response surface or machine learning techniques for broader structural applications.

5. Acknowledgment

The author sincerely acknowledges **Engr. Abdulmalik Hussaini** of the **Department of Civil Engineering, Federal University Dutsin-Ma**, for his valuable advice, encouragement, and unwavering support throughout the course of this research.

Author Contributions (CRediT Taxonomy)

Auwal Abdullahi Umar: Conceptualization, Methodology, Investigation, Data Curation, Writing – Original Draft, Writing – Review & Editing, Visualization, and Supervision.

Funding Statement

This research received no external funding.

Conflict of Interest Statement

The author declares no conflict of interest.

Data Availability Statement

The data analyzed during this study are available from the corresponding author upon reasonable request.

6. References

Abdulwahab, R., Ikotun, B. D., Raheem, A. A., Adetoro, E. A., Salihu, R., & Oribamise, O. A. (2025). Effects of cow bone ash as a partial replacement of cement in the production of concrete. *Journal of Building Pathology and Rehabilitation*, 10(2), 1-11. <https://doi.org/10.1007/s41024-025-00627-3>

ASTM International. (2015). *ASTM C127-15: Standard test method for relative density (specific gravity) and absorption of coarse aggregate*. West Conshohocken, PA: ASTM International. <https://doi.org/10.1520/C0127-15>

ASTM International. (2015). *ASTM C127-15: Standard test method for relative density (specific gravity) and absorption of coarse aggregate*. West Conshohocken, PA: ASTM International. <https://doi.org/10.1520/C0127-15>

ASTM International. (2017). *ASTM C188-17: Standard test method for density of hydraulic cement*. West Conshohocken, PA: ASTM International. <https://doi.org/10.1520/C0188-17>

ASTM International. (2019). *ASTM C618-19: Standard specification for coal fly ash and raw or calcined natural pozzolan for use in concrete*. West Conshohocken, PA: ASTM International. <https://doi.org/10.1520/C0618-19>

ASTM International. (2021). *ASTM D7348-21: Standard test methods for loss on ignition (LOI) of solid combustion residues*. West Conshohocken, PA: ASTM International. <https://doi.org/10.1520/D7348-21>

ASTM International. (2022). *ASTM C430-22: Standard test method for fineness of hydraulic cement by the 45-µm (No. 325) sieve*. West Conshohocken, PA: ASTM International. <https://doi.org/10.1520/C0430-22>

Aygörmez, Y., & Canpolat, O. (2021). Long-term sulfuric and hydrochloric acid resistance of silica fume and colemanite waste reinforced metakaolin-based geopolymers. *Revista de la construcción*, 20(2), 291-307. https://www.scielo.cl/scielo.php?pid=S0718-915X2021000200291&script=sci_arttext

Bansal, M., Bansal, M., Bahrami, A., Krishan, B., Garg, R., Özkılıç, Y. O., & Althaqafi, E. (2024). Influence of pozzolanic addition on strength and microstructure of metakaolin-based concrete. *Plos one*, 19(4), e0298761. <https://doi.org/10.1371/journal.pone.0298761>

Benjamin, M. A. Z., Ng, S. Y., Saikim, F. H., & Rusdi, N. A. (2022). The effects of drying techniques on phytochemical contents and biological activities on selected bamboo leaves. *Molecules*, 27(19), 6458. <https://doi.org/10.3390/molecules27196458>

Bhagora, F. S. (2022). Acid Rain. *International Journal of Advanced Research in Arts, Science, Engineering & Management (IJARASEM)*, 9(5), 2133-2144.

Bih, N. L., Mahamat, A. A., Chinweze, C., Ayeni, O., Bidossèssi, H. J., Onwualu, P. A., & Boakye, E. E. (2022). The effect of bone ash on the physio-chemical and mechanical properties of clay ceramic bricks. *Buildings*, 12(3), 336. <https://doi.org/10.3390/buildings12030336>

British Standards Institution. (1992). *Specification for aggregates from natural sources for concrete (BS 882:1992)*. London, United Kingdom: British Standards Institution.

British Standards Institution. (2002). *Mixing water for concrete – Specification for sampling, testing and assessing the suitability of water, including water recovered from processes in the concrete industry, as mixing water for concrete (BS EN 1008:2002)*. London, United Kingdom: British Standards Institution.

British Standards Institution. (2011). *Cement – Part 1: Composition, specifications and conformity criteria for common cements (BS EN 197-1:2011)*. London, United Kingdom: British Standards Institution.

British Standards Institution. (2013). *Aggregates for concrete (BS EN 12620:2013)*. London, United Kingdom: British Standards Institution

British Standards Institution. (2019). *BS 8500-2:2015+A2:2019 – Concrete – Complementary British Standard to BS EN 206 – Part 2: Specification for constituent materials and concrete*. London, United Kingdom: BSI.

British Standards Institution. (2019). *BS EN 12390-3:2019 – Testing hardened concrete – Part 3: Compressive strength of test specimens*. London, United Kingdom: British Standards Institution.

Filazi, A., Demir, I., & Sevim, O. (2020). Enhancement on mechanical and durability performances of binary cementitious systems by optimizing particle size distribution of fly ash. *Archives of Civil and Mechanical Engineering*, 20(2), 58. <https://doi.org/10.1007/s43452-020-00061-x>

Hosseini, M., Dolatshahi, A. R., & Ramezani, E. (2022). Effect of Acid Rain on Physical and Mechanical Properties of Concrete Containing Micro-Silica and Limestone Powder. *Journal of Mining and Environment*, 13(1), 185-200. DOI:10.22044/jme.2022.11491.2137

Ikumapayi, C. M., Omotayo, O. O., Akande, S. P., & Lawrence, R. O. (2024). EVALUATION OF RHA/BLA POZZOLANIC CEMENT CONCRETE PROPERTIES. *Journal of Civil Engineering*, 15(2), 166-178.

Karimi, Z., & Rahbar-Kelishami, A. (2024). The study of acid leaching on the mineralogical and microscopic changes of red mud. *Mining, Metallurgy & Exploration*, 41(2), 1121-1133.

Koschanin, J., Nochaiya, T., Suriwong, T., Laonamsai, J., & Julphunthong, P. (2024). Enhancing durability of concrete mixtures with supplementary cementitious materials: a study on organic acid corrosion and physical abrasion in pig farm environments. *Case Studies in Construction Materials*, 20, e02731. <https://doi.org/10.1016/j.cscm.2023.e02731>

Li, L., Liu, W., You, Q., Chen, M., & Zeng, Q. (2020). Waste ceramic powder as a pozzolanic supplementary filler of cement for developing sustainable building materials. *Journal of Cleaner Production*, 259, 120853. <https://doi.org/10.1016/j.jclepro.2020.120853>

Lu, C., Wang, W., Zhou, Q., Wei, S., & Wang, C. (2020). Mechanical behavior degradation of recycled aggregate concrete after simulated acid rain spraying. *Journal of Cleaner Production*, 262, 121237.

Luka, J., Olubajo, O. O., & Abuthakir, I. (2022). A Study on Portland Limestone Cement Blended with Animal Bone Ash and Metakaolin. *American Journal of Chemical Engineering*, 10(3), 103-115. <https://doi.org/10.11648/j.ajche.20221005.12>

Mohammed, A., Ghaithan, A., & Al-Yami, F. (2023). An integrated fuzzy-FMEA risk assessment approach for reinforced concrete structures in oil and gas industry. *Journal of Intelligent & Fuzzy Systems*, 44(1), 1129-1151. <https://doi.org/10.3233/JIFS-221328>

Mohd Nasir, N. A., Abu Bakar, N., Safiee, N. A., & Abdul Aziz, F. N. A. (2022). Permeation-durability properties of metakaolin blended concrete containing rubber. *European Journal of Environmental and Civil Engineering*, 26(11), 5113-5128. <https://doi.org/10.1080/19648189.2021.1885499>

Nayak, B., Singh, T. J., & Nayak, S. K. (2023). Study on the fretting wear behaviour of AZ91/BLA MMCs and the implications that BLA has on that behaviour. *Materials Today: Proceedings*. <https://doi.org/10.1016/j.matpr.2023.09.065>

Nochaiya, T., Suriwong, T., & Julphunthong, P. (2022). Acidic corrosion-abrasion resistance of concrete containing fly ash and silica fume for use as concrete floors in pig farm. *Case Studies in Construction Materials*, 16, e01010. <https://doi.org/10.1016/j.cscm.2022.e01010>

Onyelowe, K. C., Ebid, A. M., Awoyerwa, P., Kamchoom, V., Rosero, E., Albuja, M., & Mancheno, C. (2025). Prediction and validation of mechanical properties of self-compacting geopolymers concrete using combined machine learning methods a comparative and suitability assessment of the best analysis. *Scientific Reports*, 15(1), 6361. <https://doi.org/10.1038/s41598-025-90468-4>

Pandiyarajan, N., & Nunthavarawong, P. (2024). Recent advancements in sealants solutions for surface coatings: a comprehensive review. *Journal of Bio-and Triboro-Corrosion*, 10(3), 61.

QIU, P., MENG, E., WANG, Q., & WU, D. (2023). Erosion Resistance of Pre-Treated Rice Husk Ash Concrete Under Simulated Acid Rain. *Ceramics-Silikáty*, 67(3), 360-370. <https://doi.org/10.13168/cs.2023.0036>

Qureshi, L. A., Ali, B., & Ali, A. (2020). Combined effects of supplementary cementitious materials (silica fume, GGBS, fly ash and rice husk ash) and steel fiber on the hardened properties of recycled aggregate concrete. *Construction and Building Materials*, 263, 120636. <https://doi.org/10.1016/j.conbuildmat.2020.120636>

Shammas, N. K., Wang, L. K., & Wang, M. H. S. (2020). Sources, chemistry and control of acid rain in the environment. In *Handbook of environment and waste management: Acid rain and greenhouse gas pollution control* (pp. 1-26). https://doi.org/10.1142/9789811207136_0001

Singh, N., Varsha, S., Sai, A. R., & Sufyan-Ud-Din, M. (2022). Strength, electrical resistivity and sulfate attack resistance of blended mortars produced with agriculture waste ashes. *Case Studies in Construction Materials*, 16, e00944. <https://doi.org/10.1016/j.cscm.2022.e00944>

Temizel, C., Canbaz, C. H., Palabiyik, Y., Aydin, H., Tran, M., Ozyurtkan, M. H., ... & Johnson, P. (2021, October). A thorough review of machine learning applications in oil and gas industry. In *SPE Asia Pacific Oil and Gas Conference and Exhibition* (p. D031S025R002). SPE. <https://doi.org/10.2118/205720-MS>

Thissen, P., Bogner, A., & Dehn, F. (2024). Surface treatments on concrete: An overview on organic, inorganic and nano-based coatings and an outlook about surface modification by rare-earth oxides. *RSC Sustainability*. <https://doi.org/10.1039/D3SU00482A>

Tian, Q., Zhou, J., Hou, J., Zhou, Z., Liang, Z., Sun, M., ... & Huang, J. (2024). Building the future: Smart concrete as a key element in next-generation construction. *Construction and Building Materials*, 429, 136364. <https://doi.org/10.1016/j.conbuildmat.2024.136364>

Tipraj, B., & Shanmugapriya, T. (2023). Experimental investigation on trinary blended geopolymers mortar synthesized from Industrial-agro and municipal solid waste ash subjected to different acid exposure. *Materials Research Express*, 10(12), 125503. <https://doi.org/10.1088/2053-1591/ad112a>

Tiza, M. T., Imoni, S., Akande, E. O., Mogbo, O., Jiya, V. H., & Onuzulike, C. (2024). Revolutionizing Infrastructure Development: Exploring Cutting-Edge Advances in Civil Engineering Materials. *Recent Progress in Materials*, 6(3), 1-68. doi:10.21926/rpm.2403023

Wang, W., Shen, A., He, Z., Guo, Y., & Li, D. (2021). Mechanism and erosion resistance of internally cured concrete including super absorbent polymers against coupled effects of acid rain and fatigue load. *Construction and Building Materials*, 290, 123252. <https://doi.org/10.1016/j.conbuildmat.2021.123252>

Zerihun, B., Yehualaw, M. D., & Vo, D. H. (2022). Effect of agricultural crop wastes as partial replacement of cement in concrete production. *Advances in Civil Engineering*, 2022(1), 5648187. <https://doi.org/10.1155/2022/5648187>

Zhang, Y., Zhuang, S., Qu, M., Fang, Q., Zhao, Q., & Chen, G. (2024). Experimental study on compressive behavior of compressive stress-loaded concrete at different strain rates under simulated acid rain environment. *Journal of Building Engineering*, 96, 110584. <https://doi.org/10.1016/j.jobe.2024.110584>

Zhou, Y., Gong, G., Xi, B., Guo, M., Xing, F., & Chen, C. (2022). Sustainable lightweight engineered cementitious composites using limestone calcined clay cement (LC3). *Composites Part B: Engineering*, 243, 110183. <https://doi.org/10.1016/j.compositesb.2022.110183>